Synthesis and Characterization of Fe–Ni/Poly(methyl methacrylate) Nanocomposites

Guo-Xing Zhu, Hui-Qun Sun, Xian-Wen Wei,* Ju-Hong Zhou, Ye-Cang Tang, and Dong-Qin Zhang
College of Chemistry and Materials Science, Anhui Key Laboratory of Functional Molecular Solids, Anhui Normal University, Wuhu 241000, P. R. China

(Received August 10, 2005; CL-051039)

Spherical Fe–Ni/poly(methyl methacrylate) (PMMA) nanocomposites with diameters of 80 and 150 nm prepared on a mild condition using hydrazine as reducing agent are typical soft magnets. We anticipate that this method will lead to extensive study of the chemistry and physics of alloys/polymer spheres, which might find important applications in catalysis and magnetic storage devices.

Metal/polymer nanocomposites not only combine the advantageous properties of metals and polymers, exhibit excellent optical, electrical, catalytic, and mechanical properties[1] that single-phase material does not have, but also have potential application in catalysis, electronics and nonlinear optics.[2,3] Many methods have been developed to prepare a number of metal/polymer nanocomposites, including in situ chemical reduction, surface reaction, seeding or electroless plating, self-assembly, and infiltration.[4] A number of noble metal/polymer nanocomposites such as Ag/polymer[5–7] and Au/polymer[8,9] have been reported. However, the report for the nanocomposites of magnetic metal (Fe, Co, and Ni) or alloys with polymer is limited, only Ni/PMMA nanocomposites were obtained using radiation-induced reduction of nickel ions and radiation-inducation polymerization of methyl methacrylate (MMA) with ^{60}Co γ-rays.[10]

Fe–Ni alloy is an important soft magnetic material having high-saturation magnetization, low coercivity, low thermal expansion,[11] good anticorrosion properties,[12] lower permeability but higher electrical resistivity and having many anomalies of physical properties such as Invar[13] and Permalloy[14] anomalies. In this communication, we report firstly the synthesis of Fe–Ni/PMMA nanocomposites using chemical reduction method under moderate conditions. The route presented here is low-cost and much convenient, which may stimulate technological interests.

All reagents were analytical grade. PMMA microspheres with diameter of about 350 nm were prepared by emulsifier-free emulsion polymerization.[15] After being centrifuged and washed with water, they were dispersed in water to yield a latex dispersion of 10 wt %. For the synthesis of Fe–Ni/PMMA nanocomposites, 1.1174 g of $FeSO_4 \cdot 7H_2O$ and 1.0553 g of $NiSO_4 \cdot 6H_2O$ were dissolved in 3 cm^3 of distilled water, and then 0.5 cm^3 of PMMA solution (10 wt %) was added. After stirring for 12 min, NaOH solution (containing 1.0025 g of NaOH and 1 cm^3 of distilled water) and 17 cm^3 of ethanol were added successively. The above mixture was rapidly added to the aqueous solution containing 10 cm^3 of $N_2H_4 \cdot H_2O$ (85 wt %) and 0.9909 g of NaOH, then kept at 75 °C for about 30 min. The products were centrifugated and repeatedly washed with ethanol and distilled water, dried under vacuum at room temperature, and denoted as sample 1. Using the same procedures, when only the initial metal amounts used were reduced to half and one fourth of that in the sample 1, sample 2, and sample 3 were obtained, respectively.

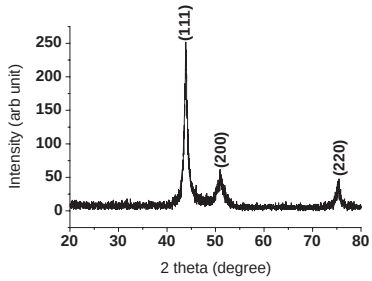

Figure 1. XRD pattern of the Fe–Ni/PMMA nanocomposites (sample 1).

All the samples obtained have similar XRD patterns. Figure 1 showed the typical XRD pattern of the sample 1, the peaks show good agreement with those of the JCPDS (No. 47-1417) data of the Fe–Ni alloy with face-centered cubic phase. The peaks at 2θ values of 43.80, 51.07, and 74.97° correspond to the Fe–Ni crystal planes of (111), (200), and (220), respectively. The broad peaks indicated that the dimension of Fe–Ni alloys nanoparticles was very small. On applying the Scherrer's equation to (111) reflection,[16] the sizes of Fe–Ni alloys nanoparticles were calculated to be about 10 nm.

TEM image of the sample 1 is shown in Figure 2A. The mean diameter of the nanocomposites is about 80 nm, which is much smaller than the original PMMA microspheres (diameter in ca. 350 nm). The decrease may be caused by the hydrolyzation and dissolution of PMMA in the reaction process. The Fe–Ni particles were spherical and homogeneously dispersed in PMMA matrices. The mean diameter of Fe–Ni nanoparticles was measured to be about 10 nm, which was in good agreement with the result of XRD analysis. The selected-area electron diffraction pattern (Figure 2B) showed the presence of diffraction

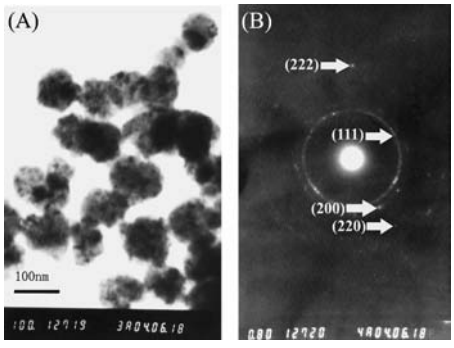

Figure 2. (A) TEM and (B) SAED images of the Fe–Ni/PMMA nanocomposites (sample 1).

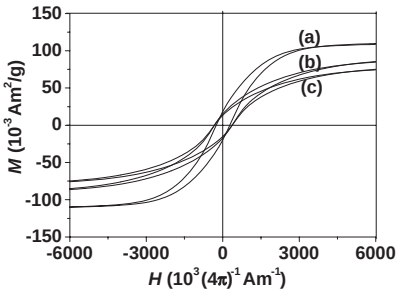

Figure 3. Hysteresis loops of (a) sample 1, (b) sample 2, and (c) sample 3.

rings corresponding to the (111), (200), (220), and (222) planes of fcc Fe–Ni alloy, indicated the polycrystalline nature of Fe–Ni alloy in the Fe–Ni/PMMA nanocomposites.

TEM images (not shown) indicated the average diameters of the nanocomposites in sample 2 have increased to about 150 nm, this may be caused by less hydrolyzation owing to lower $[M^{2+}]$. However, the spherical nanocomposites have not been formed in the sample 3, only the mixture of PMMA and isolated Fe–Ni particles with diameters of 10–80 nm were found.

The IR spectrum of Fe–Ni/PMMA nanocomposites is similar to that of free PMMA except the characteristic peak of carboxyl group at 3400 cm^{-1} has been intensified, which indicated the hydrolyzation of PMMA has taken place in the reaction process. The characteristic peak located at 1728 cm^{-1} can be attributed to C=O absorption bands, which may be produced by the dehydrogenation of ethanol on Ni.[4]

One possible mechanism of formation of the nanocomposites may be as follows. First, the surface layers of the PMMA colloids were permeated by the metal ions. Subsequently, $Fe(OH)_2 \cdot Ni(OH)_2$ was formed in situ when NaOH was introduced. Then the hydroxides in the swollen layers were reduced by $N_2H_4 \cdot H_2O$, and the swollen layers of the PMMA colloids were loaded uniformly with alloy nanoparticles.

Magnetic properties of samples were investigated at room temperature using a vibrating sample magnetometer with an applied field $-6000\ (4\pi)^{-1} \cdot kAm^{-1} < H < 6000\ (4\pi)^{-1} \cdot kAm^{-1}$. Figure 3 shows the magnetic hysteresis loops for samples 1, 2, and 3, which are the typical loops of soft magnet. Values of saturation magnetization (M_s), remanence-to-saturation ratio (M_r/M_s) and coercivity (H_c) for all samples are listed in Table 1. The M_s increased with $[M^{2+}]$ increasing probably owing to more Fe–Ni alloys in the nanocomposites. M_r/M_s of Fe–Ni/PMMA nanocomposites almost keeps constant. There was no bigger change of coercivity between sample 1 and sample 2, but that value of sample 3 is smaller than sample 1 or 2. This may be caused by the noncomposite structures, in which alloy nanoparticles have some conglomeration, causing bigger size and then decreasing the coercive force.[17]

In summary, spherical Fe–Ni/PMMA nanocomposites with diameters of 80 and 150 nm were prepared on a mild condition by a solution phase chemical reduction, which have typical soft magnetic properties. The diameter of the nanocomposites is smaller than that of the original PMMA microspheres indicated that the hydrolysis of PMMA had occurred in the course of the reduction. Fe–Ni/PMMA nanocomposites could have applications in nanoelectronics, catalysis and magnetic storage devices.

Table 1. Magnetization data for various samples measured at room temperatures

Samples No.	Hc $(4\pi)^{-1} \cdot kAm^{-1}$	Ms $10^{-3} \cdot Am^2/g$	Mr/Ms
1	268	110	0.17
2	249	99	0.16
3	174	80	0.18

We thank Anhui Provincial Excellent Young Scholars Foundation (No. 04046065), National Natural Science Foundation (Nos. 20271002 and 20490210) of P. R. China, and the State Education Ministry (EYTP, SRF for ROCS) for financial support.

References

1 D. M. Bigg, *Polym. Compos.*, **125**, 7 (1996).
2 Y. Nakao, *J. Colloid Interface Sci.*, **171**, 386 (1995).
3 J. H. Fendler and F. C. Meldrum, *Adv. Mater.*, **7**, 607 (1995).
4 D. H. Chen, J. P. Lin, S. H. Wu, and C. T. Wang, *Chem. Lett.*, **32**, 662 (2003).
5 L. M. Wang and D. J. Chen, *Chem. Lett.*, **33**, 1010 (2004).
6 Y. Zhou, S. H. Yu, C. Y. Wang, Y. R. Zhu, and Z. Y. Chen, *Chem. Lett.*, **28**, 677 (1999).
7 J. M. Lee, D. W. Kim, Y. H. Lee, and S. G. Oh, *Chem. Lett.*, **34**, 928 (2005).
8 F. K. Liu, S. Y. Hsieh, F. H. Ko, and T. C. Chu, *Colloids Surf. A*, **231**, 31 (2003).
9 Y. H. Ni, X. W. Ge, Z. C. Zhang, and Q. Ye, *Mater. Lett.*, **55**, 171 (2002).
10 Y. H. Ni, X. W. Ge, Z. C. Zhang, and Z. L. Zhu, *Chin. J. Chem. Phys.*, **15**, 393 (2002).
11 N. Grobert, M. Mayne, M. Terrones, J. Sloan, R. E. Dunin-Borkwski, R. Kamalakaran, T. Seeger, H. Terrones, N. Rühle, D. M. R. Walton, H. W. Kroto, and J. L. Hutchison, *Chem. Commun.*, **2001**, 471.
12 R. Bolsoni, V. Drago, and E. Lima Jr., *J. Metastable and Nanocryst. Mater.*, **14**, 51 (2002).
13 S. Kumar, K. Roy, K. Maity, T. P. Sinha, D. Banerjee, K. C. Das, and R. Bhattacharya, *Phys. Status Solidi A*, **167**, 175 (1998).
14 S. U. Jen, S. P. Shieh, and S. S. Liou, *J. Magn. Magn. Mater.*, **147**, 49 (1995).
15 Y. C. Tang, S. Z. Lou, and Y. M. Sun, *Chin. J. Synth. Chem.*, **10**, 324 (2002).
16 C. N. J. Wagner and E. N. Aqua, *Adv. X-Ray Anal.*, **7**, 46 (1964).
17 C. Kuhrt and L. Schultz, *J. Appl. Phys.*, **73**, 6588 (1993).

Published on the web (Advance View) November 19, 2005; DOI 10.1246/cl.2005.1680